THE JOURNAL OF PHYSICAL CHEMISTRY LETTERS
A JOURNAL OF THE AMERICAN CHEMICAL SOCIETY

pubs.acs.org/JPCL

Letter

Sulfur Dioxide Sulfide (SSO_2): The Elusive Isovalent Analogue of Sulfur Trioxide (SO_3)

Mason McAnally, Xilin Bai, Yuheng Luo, Zesen Wang, Jinghui Lu, Ashanie Herath, Chaojiang Zhang, Jia Wang, Andrew M. Turner, Baoyu Song, Yang Pan,* Tao Yang,* Rui Sun,* Ryan C. Fortenberry,* and Ralf I. Kaiser*

Cite This: *J. Phys. Chem. Lett.* 2026, 17, 13415−13420

Read Online

ACCESS | Metrics & More | Article Recommendations | Supporting Information

ABSTRACT: Sulfur dioxide sulfide (SSO_2) has remained experimentally undetected despite repeated theoretical predictions of its stability. As a missing sulfur oxide isovalent to sulfur trioxide (SO_3), SSO_2 occupies a distinctive position at the boundary of formally hypervalent bonding, where replacing oxygen with sulfur perturbs a delocalized chalcogen-oxide framework. Here, we close this long-standing gap by identifying SSO_2 in cryogenic SO_2 ices processed by energetic electrons using tunable vacuum ultraviolet photoionization reflectron time-of-flight mass spectrometry and high-level quantum chemical computations. These studies reveal a broader sulfur oxide network including sulfur oxide peroxide (OSOO), 1,2,3-dioxathiirane 3-oxide (cyclic-S(O)OO), and disulfur monoxide (S_2O). Our results establish sulfur-atom incorporation into SO_2 as a viable condensed-phase route to a previously elusive sulfur oxide—SSO_2—and highlight its unique molecular structure in sulfur-rich planetary and astrochemical environments.

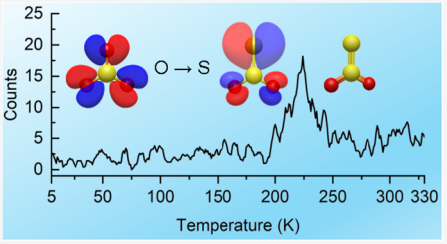

Trigonal planar (D_{3h}) sulfur trioxide (SO_3; **3a**, Figure 1) serves as the prototypical hypervalent sulfur oxide and a benchmark system for delocalized π bonding. Although commonly depicted as a trigonal planar molecule with three sulfur−oxygen double bonds (S═O),[1−3] its electronic structure is more accurately described by a symmetry-delocalized π system extending over the entire molecular framework. The extent to which such delocalization persists under isovalent heteroatom substitution, however, remains unresolved. Substitution of a single oxygen by sulfur yields trigonal planar sulfur dioxide sulfide (SSO_2; **1a**, Figure 1), a heavier isovalent analogue of sulfur trioxide (SO_3; **3a**) that preserves valence electron count while lowering molecular symmetry and perturbing the π manifold. This oxygen → sulfur (O→S) substitution provides a direct probe of how heteroatom replacement perturbs π delocalization, bond polarity, and hypervalent bonding in chalcogen oxides.[3]

Despite being predicted computationally as a local minimum on the sulfur oxide potential energy surface,[4−7] SSO_2 (**1a**) has eluded experimental detection, unlike SO_3 and a broader family of disulfur dioxide isomers (cis-/trans-/cyclic-OSSO and OSOS).[8−11] This persistent absence poses a fundamental gap in sulfur oxide chemistry with direct relevance to the chemistry of sulfur-rich environments extending from atmospheric and geochemical[12−15] to astrophysical environments such as cold molecular clouds (TMC-1),[16−19] carbonaceous asteroids like Ryugu[20,21] and Bennu,[22] Venus,[23−25] and Io,[26] where isomer distributions govern reaction branching, isotope fractionation, and sulfur speciation.

Here, we synthesize and identify sulfur dioxide sulfide (SSO_2; **1a**) in cryogenically processed sulfur dioxide (SO_2) ices at 5 K under ultrahigh vacuum conditions (10^{-11} Torr) driven by nonequilibrium chemistry. Exploiting time-resolved Fourier transform infrared (FTIR) spectroscopy, temperature-programmed desorption (TPD), and tunable vacuum ultraviolet (VUV) photoionization reflectron time-of-flight mass spectrometry (PI-ReToF-MS), supported by high-level electronic structure calculations, we detect the previously elusive SSO_2 (**1a**) along with additional sulfur oxides such as sulfur trioxide (SO_3; **3a**), sulfur oxide peroxide (OSOO; **3b**), 1,2,3-dioxathiirane 3-oxide (cyc-S(O)OO; **3c**), and disulfur monoxide (S_2O; **6a**) (see Supporting Information) accessible via excited state and/or nonadiabatic reaction dynamics. These results establish sulfur atom addition into SO_2 as a viable route to SSO_2 **1a** providing access to symmetry reduced bonding frameworks.

Reflectron time-of-flight mass spectrometry (ReToF-MS) coupled with soft photoionization techniques allows for discrimination of isomeric species based on adiabatic ionization energies (IEs). These adiabatic ionization energies are determined using high-level *ab initio* quantum chemical

Received: September 30, 2026
Revised: October 28, 2026
Accepted: October 29, 2026
Published: November 4, 2026



ACS Publications © 2026 American Chemical Society

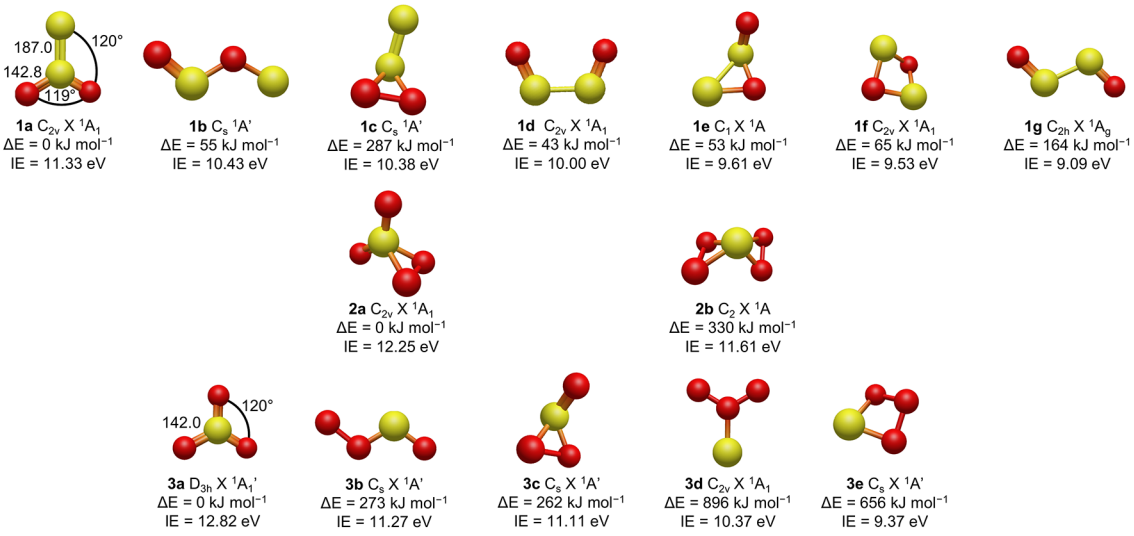

Figure 1. Computed structures of sulfur oxide isomers of S_2O_2 (**1**), SO_4 (**2**), and SO_3 (**3**) along with adiabatic ionization energies (IEs), point groups, ground electronic states, and relative energies (ΔE) calculated at the CCSD(T)-F12/cc-pVTZ-F12 level of theory with zero-point energies (ZPEs). Bond units are in pm.

calculations capable of accurately and precisely predicting ionization thresholds of each molecule within an error of ± 0.05 eV. The IEs calculated here show an average error of 0.01 eV against available experimental IEs (Table S1).[27−29] Additional sulfur oxides and their adiabatic IEs were explored for sulfur monoxide (SO), sulfur dioxide (SO_2), sulfur trioxide (SO_3), and disulfur monoxide (S_2O) (Figure S1, Table S1). Based on these calculations, experiments were conducted utilizing specific energies from 10.20 to 13.00 eV (Figure 2;

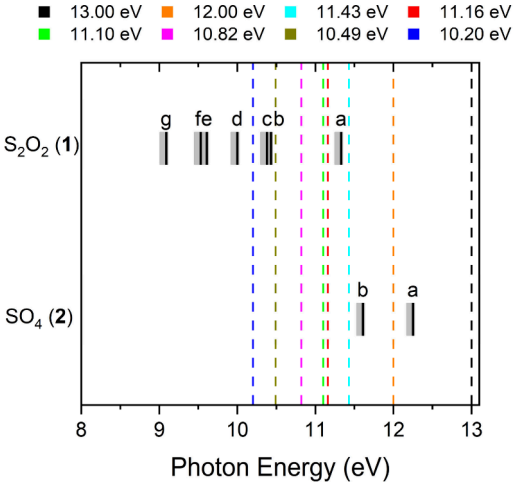

Figure 2. Compilation of ionization energies of the S_2O_2 and SO_4 isomers corrected for computational error and the Stark effect (gray bars) along with photon energies used in the experiments (dashed colored lines).

Table S2; Figure S2). Experiments from 11.16 to 13.00 eV were completed utilizing synchrotron vacuum ultraviolet light, while lower photon energies utilized four-wave mixing techniques (Table S3). For a full-range mass spectrum collected during TPD at 12.00 eV see Figure S3.

Measurements at three photon energies were conducted to determine the presence of signal observed at m/z = 96. Each experiment signal at 12.00 and 11.43 eV were summed over three replicate experiments. This mass can be attributed to two formulas: SO_4 (**2**) and S_2O_2 (**1**). Using a photon energy of 12.00 eV, SO_4 (**2b**) and all isomers of S_2O_2 (**1a−1g**) can be ionized (Figure 2); a sublimation event is recorded peaking at 225 K (Figure 3). Tuning to 11.43 eV, SO_4 (**2b**) can no longer

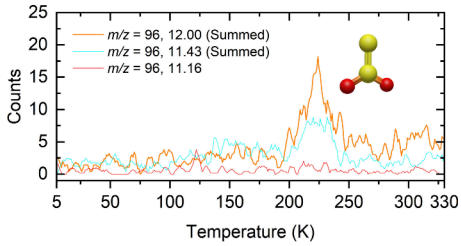

Figure 3. TPD-ReToF-MS profile of the irradiated sulfur dioxide ice at m/z = 96. TPD profiles collected at photon energies of 12.00 eV (orange), 11.43 eV (cyan), and 11.16 eV (red) are depicted.

be ionized; however, the peak remains at 225 K with diminished signal. The drop of the ion signal could be attributed to SO_4 (**2b**) subliming or to a drop in ionization efficiency of S_2O_2 (**1a**). Next, the photon energy is tuned to 11.16 eV, at which only S_2O_2 **1b−1g** can be ionized, but not SSO_2 **1a**. No signal was recorded at 11.16 eV; thus, the signal observed at 11.43 eV can originate only from SSO_2 **1a**.

These measurements provide the first experimental detection of SSO_2 **1a**, a compound thought to exist in Venus' atmosphere.[23] However, atmospheric modeling studies indicate that recombination of sulfur monoxide is barriered toward SSO_2 **1a** formation, limiting generation under atmospheric conditions. Alternatively, direct addition of atomic sulfur to SO_2 may provide a route to SSO_2 **1a**.

The formation of S_2O_2 has been highly sought after due to its theorized role in atmospheric and astrophysical contexts.[7,23,24] To provide insight into the reaction mechanism governing SSO_2 formation, electronic structure calculations were performed at the XMS-CASPT2(8,8)/def2-TZVPPD//ωB97X-D4/def2-TZVPPD level of theory (Supporting Information). These computations provide direct insight into the

https://doi.org/10.1021/acs.jpclett.6c03291
J. Phys. Chem. Lett. 2026, 17, 13415−13420

energetics of the reactants, transition states, intermediates and products with an expected accuracy of ± 5 kJ mol^{-1}. In detail, we explore the reaction of atomic sulfur in the ^{3}P ground state and ^{1}D excited state with SO_2 on the triplet and singlet potential energy surfaces (Figure 4).

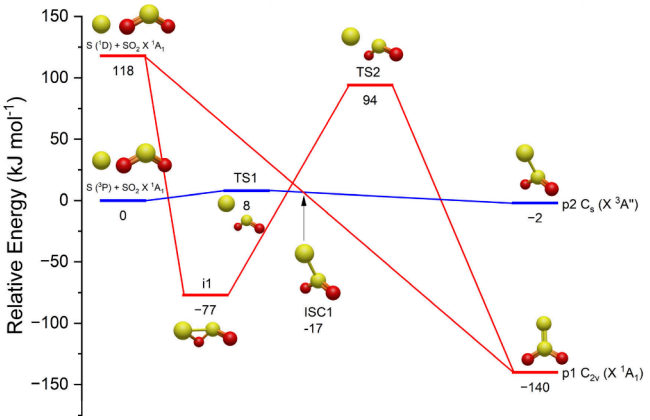

Figure 4. Calculated potential energy surface of atomic sulfur (S, ^{3}P/^{1}D) reacting with sulfur dioxide (SO_2, X $^1A_1$) on the triplet and singlet manifolds toward the formation of S_2O_2 isomers computed with XMS-CASPT2(8,8)/def2-TZVPPD//ωB97X-D4/def2-TZVPPD with zero-point energies (ZPEs).

On the triplet surface (Figure 4, blue), the reaction of ground state atomic sulfur with SO_2 (X $^1A_1$) proceeds through a low-lying transition state (**TS1**) located 8 kJ mol^{-1} above the separated reactants and results in the formation of nonplanar triplet SSO_2 **p2** (C_s, X ^{3}A"). This addition to the sulfur atom is exoergic by 2 kJ mol^{-1}. This product is 138 kJ mol^{-1} above the singlet SSO_2 **p1**.

Alternatively, the singlet surface contains two pathways to product formation. To form **i1**, singlet sulfur (^{1}D) undergoes cycloaddition to the sulfur and oxygen of sulfur dioxide forming a three membered ring intermediate. The latter isomerizes through a barrier of 171 kJ mol^{-1} via ring-opening before generating SSO_2 **p1**. This overall reaction from singlet sulfur to **i1** → **TS2** → **p1** is exoergic by 258 kJ mol^{-1}. Alternatively, the singlet sulfur can add to the sulfur atom of sulfur dioxide resulting in **p1** in one step. The stronger spin−orbit coupling of sulfur relative to oxygen increases the likelihood of intersystem crossing. After **TS1**, the singlet and triplet potential energy surfaces approach one another at the intersystem crossing point, **ISC1** (−17 kJ mol^{-1}), providing access to SSO_2 **p1** through nonadiabatic dynamics. Although this reaction likely proceeds via sulfur addition to SO_2, warming during TPD may facilitate additional product formation or increased diffusion of reactive species.

The detection of sulfur dioxide sulfide (SSO_2; **1a**) together with sulfur oxide peroxide (OSOO; **3b**), cyclic-sulfur trioxide (**3c**), and disulfur monoxide (S_2O; **6a**) (see Supporting Information) demonstrates that electron-driven processing of pure sulfur dioxide ice generates a broader sulfur oxide inventory than is apparent from infrared spectroscopy alone.[30,31] Whereas FTIR (Supporting Information) predominantly reveals the accumulation of sulfur trioxide (SO_3; **3a**) and, through sequential association, the polymeric phase of sulfur trioxide (γ-SO_3) (Figure S4, Table S4), tunable PI-ReToF-MS exposes additional transients released during TPD. Time-resolved FTIR fitting (Figure S5, Table S5) shows that SO_2 is consumed through dissociation and disproportionation pathways that generate SO and SO_3. These kinetics establish SO_3 as the dominant bulk infrared-active product, while the absence of SSO_2 **1a**, OSOO **3b**, cyclic-S(O)OO **3c**, and S_2O **6a** from the FTIR spectra is consistent with abundances below the infrared detection limit. Previous studies on SO_2-bearing ices have utilized only FTIR and were systematically unable to detect minor products critical to branching ratios for oxosulfur compounds.[31−34]

Finally, the electronic structure calculations provide a mechanistic basis for the formation of SSO_2 **1a** under these nonequilibrium conditions. On the triplet surface, sulfur atom addition to SO_2 proceeds through a low-lying transition state to a triplet adduct, which can undergo intersystem crossing to SSO_2 **1a**. On the singlet surface, S(^{1}D) addition to SO_2

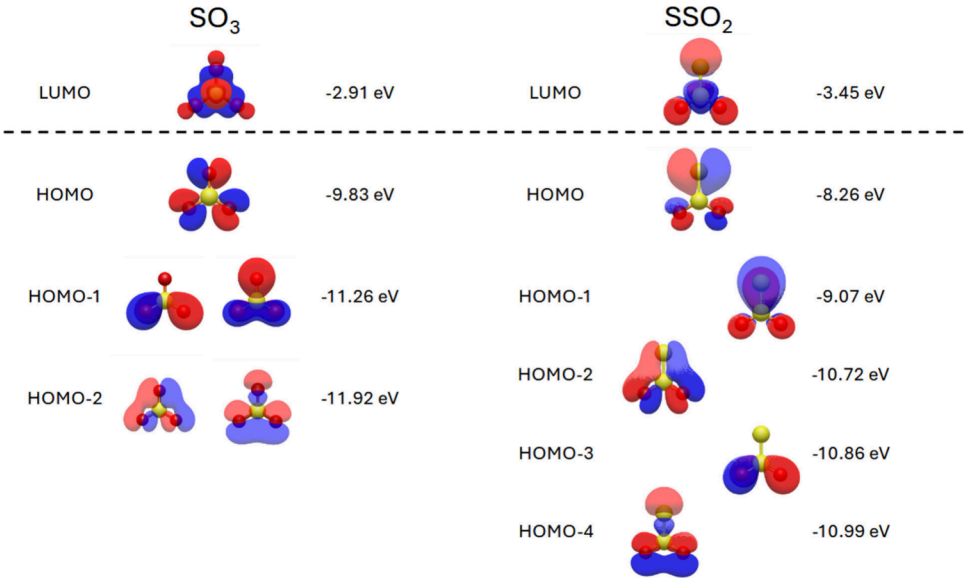

Figure 5. Calculated frontier molecular orbitals (MOs) and electronic energies of SO_3 (**3a**) and SSO_2 (**1a**) at the B3LYP/aug-cc-pVTZ level of theory. MOs visualized using Avogadro2.

https://doi.org/10.1021/acs.jpclett.6c03291
J. Phys. Chem. Lett. 2026, 17, 13415−13420

accesses either a cycloaddition to ring opening sequence or a one-step pathway. Together, these results show that SSO_2 **1a** is a chemically accessible product of sulfur atom addition chemistry in cryogenic sulfur dioxide ices. Although SSO_2 **1a** is the global minimum on the isomeric potential energy surface, the previous lack of detection in SO_2 ices may reflect kinetic limitations associated with the sulfur addition and requisite nonadiabatic dynamics, causing low abundances and, thus, difficulty in detection by conventional infrared spectroscopy.[30−32]

Having identified sulfur dioxide sulfide (SSO_2; **1a**), we now explore the chemical bonding. Natural bond orbital (NBO) analyses were performed to compare the localized bonding descriptions of SO_3 (**3a**; Table S6) and SSO_2 (**1a**; Table S7) (Table S8). In SO_3, NBO identifies a localized S−O π component strongly polarized toward oxygen, with oxygen contributing 75% of the bonding orbital and sulfur contributing 25%. The remaining π density is distributed through occupied oxygen-centered *p* character, including both bonding- and antibonding-type O/O arrangements. Together, these orbitals describe a delocalized π framework across SO_3 (D_{3h}) consistent with π bonding distributed over the molecular scaffold rather than confined to independent localized S═O double bonds. By contrast, in SSO_2 (**1a**), the O→S substitution reorganizes this bonding pattern. The NBO calculation localizes the principal π component along the S−S linkage, giving nearly fully occupied σ(S−S) and π(S−S) orbitals, while the two S−O linkages are represented as polarized σ bonds, with oxygen contributing 65% and sulfur contributing 35%. This redistribution indicates that replacement of one terminal oxygen by sulfur lowers the symmetry of the π framework and shifts multiple-bond character away from S−O bonding toward the S−S linkage.

The molecular orbitals (MOs; Figure 5) reveal that under O→S substitution, the qualitative orbital framework remains the same. Even though the highest occupied molecular orbital (HOMO) remains the same, the SO_3 HOMO−1, for instance, splits with one portion of the SSO_2 HOMO−1 rising in energy more than its counterpart such that the former HOMO−2 components become interspersed within the energies of the former HOMO−1 manifold. These MOs highlight electronic structure reorganization induced by sulfur substitution. This altered bonding and orbital picture is consistent with the slightly elongated S−O bonds in SSO_2 relative to SO_3, 142.8 pm versus 142.0 pm, respectively, reflecting diminished S−O π participation upon O→S substitution. Thus, SSO_2 is not simply an isovalent analogue of SO_3 with equivalent S−O delocalization, but a lower-symmetry sulfur oxide in which the π system is redistributed toward S−S multiple bond character.[33]

Overall, electron processing of sulfur dioxide ices at cryogenic temperatures produces a substantially richer sulfur oxide chemistry than indicated by FTIR alone. While sulfur trioxide is the dominant bulk product, PI-ReToF-MS reveals additional minor isomeric channels, including sulfur dioxide sulfide (SSO_2). Supported by multireference electronic structure calculations, these data show that sulfur atom addition to the sulfur atom of sulfur dioxide, aided by excited state dynamics and/or intersystem crossing, can provide a viable condensed-phase route to this previously elusive sulfur oxide. More broadly, threshold photoionization mass spectrometry provides a general strategy for isomer-selective identification of previously elusive molecules. These results close a long-standing gap in sulfur oxide chemistry and suggest that sulfur-rich ices in astrochemical and planetary environments can host a broader inventory of transient sulfur oxide isomers than previously recognized.

■ ASSOCIATED CONTENT

Data Availability Statement

The data supporting the findings of this study are available within the Article and its Supporting Information. Additional data are available from the corresponding authors upon reasonable request.

Supporting Information

The Supporting Information is available free of charge at https://pubs.acs.org/doi/10.1021/acs.jpclett.6c03291.

Experimental details, computational methods, ionization energies, kinetic analysis, additional mass spectrometry results, NBO analysis, PES calculations, calculated geometries, calculated frequencies (PDF)

■ AUTHOR INFORMATION

Corresponding Authors

Yang Pan − *National Synchrotron Radiation Laboratory, University of Science and Technology of China, Hefei, Anhui 230029, P. R. China;* orcid.org/0000-0002-9360-3809; Email: panyang@ustc.edu.cn

Tao Yang − *State Key Laboratory of Precision Spectroscopy, East China Normal University, Shanghai 200062, P. R. China; Xinjiang Key Laboratory of Radio Astrophysics, Urumqi, Xinjiang 830011, P. R. China; Collaborative Innovation Center of Extreme Optics, Shanxi University, Taiyuan, Shanxi 030006, P. R. China;* orcid.org/0000-0003-4101-2385; Email: tyang@lps.ecnu.edu.cn

Rui Sun − *Department of Chemistry, University of Hawaii at Mānoa, Honolulu, Hawaii 96822, United States;* orcid.org/0000-0003-0638-1353; Email: ruisun@hawaii.edu

Ryan C. Fortenberry − *Department of Chemistry & Biochemistry, University of Mississippi, Oxford, Mississippi 38677, United States;* orcid.org/0000-0003-4716-8225; Email: r410@olemiss.edu

Ralf I. Kaiser − *Department of Chemistry and W.M. Keck Laboratory in Astrochemistry, University of Hawaii at Mānoa, Honolulu, Hawaii 96822, United States;* orcid.org/0000-0002-7233-7206; Email: ralfk@hawaii.edu

Authors

Mason McAnally − *Department of Chemistry and W.M. Keck Laboratory in Astrochemistry, University of Hawaii at Mānoa, Honolulu, Hawaii 96822, United States;* orcid.org/0009-0000-7799-9914

Xilin Bai − *State Key Laboratory of Precision Spectroscopy, East China Normal University, Shanghai 200062, P. R. China*

Yuheng Luo − *Department of Chemistry, University of Hawaii at Mānoa, Honolulu, Hawaii 96822, United States;* orcid.org/0000-0002-3124-1179

Zesen Wang − *Department of Chemistry and W.M. Keck Laboratory in Astrochemistry, University of Hawaii at Mānoa, Honolulu, Hawaii 96822, United States*

Jinghui Lu − *National Synchrotron Radiation Laboratory, University of Science and Technology of China, Hefei, Anhui 230029, P. R. China*
Ashanie Herath − *Department of Chemistry and W.M. Keck Laboratory in Astrochemistry, University of Hawaii at Mānoa, Honolulu, Hawaii 96822, United States*
Chaojiang Zhang − *Department of Chemistry and W.M. Keck Laboratory in Astrochemistry, University of Hawaii at Mānoa, Honolulu, Hawaii 96822, United States*
Jia Wang − *Department of Chemistry and W.M. Keck Laboratory in Astrochemistry, University of Hawaii at Mānoa, Honolulu, Hawaii 96822, United States;* Present Address: College of Engineering Physics, Shenzhen Technology University, Shenzhen 518118, China
Andrew M. Turner − *Department of Chemistry and W.M. Keck Laboratory in Astrochemistry, University of Hawaii at Mānoa, Honolulu, Hawaii 96822, United States*
Baoyu Song − *National Synchrotron Radiation Laboratory, University of Science and Technology of China, Hefei, Anhui 230029, P. R. China*

Complete contact information is available at: https://pubs.acs.org/10.1021/acs.jpclett.6c03291

Author Contributions

○M.M. and X.B. contributed equally to this work. M.M. and X.B. performed experiments. Z.W., J.L., A.H., C.Z., J.W., A.M.T., B.S., and Y.P. assisted with experiments. Y.L. and R.C.F. performed calculations. M.M., R.C.F., Y.L., and R.I.K. contributed to discussion and data analysis. M.M., R.I.K., and R.C.F. wrote the manuscript, which was edited and revised by all coauthors.

Notes

The authors declare no competing financial interest.

■ ACKNOWLEDGMENTS

This work was conducted under a Memorandum of Understanding between the East China Normal University (ECNU), the University of Hawai'i at Mānoa (UHM), and the National Synchrotron Radiation Laboratory (NSRL) at the University of Science and Technology of China (USTC). The UHM team was supported by the US National Science Foundation (NSF) Division for Astronomy (NSF-AST 2403867). R.C.F. acknowledges funding from the US National Science Foundation (NSF) Division for Astronomy (AST-2407815) and computational support from the Mississippi Center for Supercomputing Research. The ECNU team was supported by the National Natural Science Foundation of China (Grant Nos. 92461301, 12274140, 12034008, and 12250003), the Xinjiang Tianchi Talent Program (2023), and the Program for Professor of Special Appointment (Eastern Scholar) at Shanghai Institutions of Higher Learning. The advanced computing resources Koa from the University of Hawai'i Information Technology Services are gratefully acknowledged.

■ REFERENCES

(1) Gillespie, R. J.; Robinson, E. A. The sulphur−oxygen bond in sulphuryl and thionyl compounds: Correlation of stretching frequencies and force constants with bond lengths, bond angles, and bond orders. *Can. J. Chem.* **1963**, *41*, 2074−2085.
(2) Magnusson, E. Hypercoordinate molecules of second-row elements: d functions or d orbitals? *J. Am. Chem. Soc.* **1990**, *112*, 7940−7951.
(3) Denehy, E.; White, J. M.; Williams, S. J. Electronic Structure of the Sulfonyl and Phosphonyl Groups: A Computational and Crystallographic Study. *Inorg. Chem.* **2007**, *46*, 8871−8886.
(4) Marsden, C. J.; Smith, B. J. An ab initio study of many isomers of S_2O_2. A combined theoretical and experimental analysis of the harmonic force field and molecular structure of cis-planar OSSO. *Chem. Phys.* **1990**, *141*, 335−353.
(5) Ramírez-Solís, A.; Jolibois, F.; Maron, L. Born−Oppenheimer DFT molecular dynamics studies of S_2O_2: Non-harmonic effects on the lowest energy isomers. *Chem. Phys. Lett.* **2011**, *510*, 21−26.
(6) Murakami, Y.; Onishi, S.; Kobayashi, T.; Fujii, N.; Isshiki, N.; Tsuchiya, K.; Tezaki, A.; Matsui, H. High Temperature Reaction of S + SO_2 → SO + SO: Implication of S_2O_2 Intermediate Complex Formation. *J. Phys. Chem. A* **2003**, *107*, 10996−11000.
(7) Hochlaf, M.; Linguerri, R.; Cheraki, M.; Ayari, T.; Ben Said, R.; Feifel, R.; Chambaud, G. $S_2O_2^{q+}$ (q = 0, 1, and 2) Molecular Systems: Characterization and Atmospheric Planetary Implications. *J. Phys. Chem. A* **2021**, *125*, 1958−1971.
(8) Wu, Z.; Wan, H.; Xu, J.; Lu, B.; Lu, Y.; Eckhardt, A. K.; Schreiner, P. R.; Xie, C.; Guo, H.; Zeng, X. The near-UV absorber OSSO and its isomers. *Chem. Commun.* **2018**, *54*, 4517−4520.
(9) Lovas, F. J.; Tiemann, E.; Johnson, D. R. Spectroscopic studies of the SO_2 discharge system. II. Microwave spectrum of the SO dimer. *J. Chem. Phys.* **1974**, *60*, 5005−5010.
(10) Field, T. A.; Slattery, A. E.; Adams, D. J.; Morrison, D. D. Experimental observation of dissociative electron attachment to S_2O and S_2O_2 with a new spectrometer for unstable molecules. *J. Phys. B: At., Mol. Opt. Phys.* **2005**, *38*, 255-264.
(11) Herron, J. T.; Huie, R. E. Rate constants at 298 K for the reactions SO + SO + M → $(SO)_2$ + M and SO + $(SO)_2$ → SO_2 + S_2O. *Chem. Phys. Lett.* **1980**, *76*, 322−324.
(12) Liu, T.; Chan, A. W.; Abbatt, J. P. Multiphase oxidation of sulfur dioxide in aerosol particles: Implications for sulfate formation in polluted environments. *Environ. Sci. Technol.* **2021**, *55*, 4227−4242.
(13) McLinden, C. A.; Fioletov, V.; Shephard, M. W.; Krotkov, N.; Li, C.; Martin, R. V.; Moran, M. D.; Joiner, J. Space-based detection of missing sulfur dioxide sources of global air pollution. *Nat. Geosci.* **2016**, *9*, 496−500.
(14) Long, B.; Xia, Y.; Zhang, Y.-Q.; Truhlar, D. G. Kinetics of sulfur trioxide reaction with water vapor to form atmospheric sulfuric acid. *J. Am. Chem. Soc.* **2023**, *145*, 19866−19876.
(15) Holland, H. D. The oxygenation of the atmosphere and oceans. *Philos. Trans. R. Soc., B* **2006**, *361*, 903−915.
(16) McAnally, M.; Bocková, J.; Herath, A.; Turner, A. M.; Meinert, C.; Kaiser, R. I. Abiotic formation of alkylsulfonic acids in interstellar analog ices and implications for their detection on Ryugu. *Nat. Commun.* **2024**, *15*, 4409.
(17) Herath, A.; McAnally, M.; Turner, A. M.; Wang, J.; Marks, J. H.; Fortenberry, R. C.; Garcia-Alvarez, J. C.; Gozem, S.; Kaiser, R. I. Missing interstellar sulfur in inventories of polysulfanes and molecular octasulfur crowns. *Nat. Commun.* **2025**, *16*, 5571.
(18) Lique, F.; Cernicharo, J.; Cox, P. The excitation of SO in cold molecular clouds: TMC-1. *Astrophys. J.* **2006**, *653*, 1342−1352.
(19) Cernicharo, J.; Cabezas, C.; Agúndez, M.; Tercero, B.; Pardo, J.; Marcelino, N.; Gallego, J.; Tercero, F.; López-Pérez, J.; De Vicente, P. TMC-1, the starless core sulfur factory: Discovery of NCS, HCCS, H_2CCS, H_2CCCS, and C_4S and detection of C_5S. *Astron. Astrophys.* **2021**, *648*, L3.
(20) Yoshimura, T.; Takano, Y.; Naraoka, H.; Koga, T.; Araoka, D.; Ogawa, N. O.; Schmitt-Kopplin, P.; Hertkorn, N.; Oba, Y.; Dworkin, J. P.; et al. Chemical evolution of primordial salts and organic sulfur molecules in the asteroid 162173 Ryugu. *Nat. Commun.* **2023**, *14*, 5284.
(21) Harrison, C.; King, A.; Jones, R.; Russell, S. S.; Nakamura, T.; Yurimoto, H.; Noguchi, T.; Okazaki, R.; Yabuta, H.; Naraoka, H.; et al. Iron and copper sulfides in asteroid (162173) Ryugu: Formation conditions and a comparison to the CI and CY chondrites. *Meteorit. Planet. Sci.* **2025**, *60*, 506−528.

(22) Zega, T. J.; McCoy, T. J.; Russell, S. S.; Keller, L. P.; Gainsforth, Z.; Singerling, S. A.; Manga, V. R.; Harrison, C.; Libourel, G.; Prince, B. S.; et al. Mineralogical evidence for hydrothermal alteration of Bennu samples. *Nat. Geosci.* **2025**, *18*, 832−839.
(23) Frandsen, B. N.; Farahani, S.; Vogt, E.; Lane, J. R.; Kjaergaard, H. G. Spectroscopy of OSSO and Other Sulfur Compounds Thought to be Present in the Venus Atmosphere. *J. Phys. Chem. A* **2020**, *124*, 7047−7059.
(24) Krasnopolsky, V. A. Disulfur dioxide and its near-UV absorption in the photochemical model of Venus atmosphere. *Icarus* **2018**, *299*, 294−299.
(25) Vandaele, A. C.; Korablev, O.; Belyaev, D.; Chamberlain, S.; Evdokimova, D.; Encrenaz, T.; Esposito, L.; Jessup, K. L.; Lefèvre, F.; Limaye, S.; et al. Sulfur dioxide in the Venus atmosphere: II. Spatial and temporal variability. *Icarus* **2017**, *295*, 1−15.
(26) Trumbo, S. K.; Davis, M. R.; Cassese, B.; Brown, M. E. Spectroscopic Mapping of Io's Surface with HST/STIS: SO_2 Frost, Sulfur Allotropes, and Large-scale Compositional Patterns. *Planet. Sci. J.* **2022**, *3*, 272.
(27) Wang, J.; Turner, A. M.; Marks, J. H.; Fortenberry, R. C.; Kaiser, R. I. Formation of Paraldehyde ($C_6H_{12}O_3$) in Interstellar Analog Ices of Acetaldehyde Exposed to Ionizing Radiation. *ChemPhysChem* **2024**, *25*, No. e202400837.
(28) Wang, J.; Turner, A. M.; Marks, J. H.; Zhang, C.; Kleimeier, N. F.; Bergantini, A.; Singh, S. K.; Fortenberry, R. C.; Kaiser, R. I. Preparation of Acetylenediol (HOCCOH) and Glyoxal (HCOCHO) in Interstellar Analog Ices of Carbon Monoxide and Water. *Astrophys. J.* **2024**, *967*, 79.
(29) Wang, J.; Marks, J. H.; Fortenberry, R. C.; Kaiser, R. I. Interstellar formation of glyceric acid [$HOCH_2CH(OH)COOH$]-The simplest sugar acid. *Sci. Adv.* **2024**, *10*, No. eadl3236.
(30) Martín-Doménech, R.; Escribano, B.; Navarro-Almaida, D.; Taillard, A.; Carrascosa, H.; Muñoz Caro, G. M.; Fuente, A. Photodesorption of SO_2 and SO from UV-irradiated SO_2 ices. *Mon. Not. R. Astron. Soc.* **2025**, *541*, 2992−3007.
(31) Moore, M. H. Studies of proton-irradiated SO_2 at low temperatures: Implications for Io. *Icarus* **1984**, *59*, 114−128.
(32) Mifsud, D. V.; et al. Energetic electron irradiations of amorphous and crystalline sulphur-bearing astrochemical ices. *Front. Chem.* **2022**, *10*, No. 1003163.
(33) Hanwell, M. D.; Hutchison, G. R. Avogadro2, version 2.0.0; Zenodo, 2026.
(34) Kaňuchová, Z.; Boduch, P.; Domaracka, A.; Palumbo, M. E.; Rothard, H.; Strazzulla, G. Thermal and energetic processing of astrophysical ice analogues rich in SO_2. *A&A* **2017**, *604*, A68.

https://doi.org/10.1021/acs.jpclett.6c03291
J. Phys. Chem. Lett. 2026, 17, 13415−13420